Supplementary Information

A. Detailed Methods

Reagents and antibodies

Fetal bovine serum (FBS) was purchased from Hyclone and all other cell culture reagents were from Life Technologies (Carlsbad, CA). Alexa Flour568-labeled phalloidin and HCS CellMask blue were obtained from Life Technologies (Carlsbad, CA), anti-paxillin antibody clone Y113 was from Millipore (Billerica, MA), polyclonal goat anti-Synaptopodin (synpo) antibody P-19 (SC-21537) was from Santa Cruz (Dallas, TX), anti-vinculin antibody clone hvin was from Sigma-Aldrich (St. Louis, MO), anti-podocin antibody was from Santa Cruz (Dallas, TX), hamster anti-total β1 integrin antibody HMB1-1 was from BioLegend (San Diego, CA), rat anti-mouse active integrin β1 antibody 9EG7[1] was from BD Biosciences (San Jose, CA) and mouse anti-human active integrin β1 antibody 12G10[2] was from Abcam (Cambridge, MA). Rat tail Collagen I, puromycin aminonucleoside (PAN), lipopolysaccharide (LPS), mizoribine (MZR) and dexamethasone (DEX) were from Sigma-Aldrich (St. Louis, MO). Pyrintegrin (pyr) was from EMD Millipore (Billerica, MA).

Animals

Animal care and procedures were approved by the Institutional Animal Care and Use Committee (IACUC) and were performed in accordance with institutional guidelines. The C57BL/6J (B6) wild-type mice and Sprague-Dawley (SD) wild type rats were purchased from The Jackson Laboratory.

Cell lines and tissue culture

Immortalized human and murine podocytes have been described and were cultured according to published protocols,[3, 4] with slight modification. Briefly, the cells were thermo-shifted from 33°C to 37°C to induce differentiation, as described in the published protocols, and were cultured in large tissue culture flasks at 37°C for 7 days, trypsinized, re-seeded in collagen I coated multi-well plates and further cultured at 37°C in the multi-well plates for 4 days prior to use in the HCS assay.

Podocyte high-content screening assay

For the primary screen, podocytes were cultured in 96-well optical plates (PerkinElmer, Waltham, MA). Cells were typically treated with various agents, such as puromycin aminonucleoside (PAN), mizoribine (MZR), or LPS in cell culture media for 48h at 37°C. Subsequently, cells were rinsed with phosphate buffered saline (PBS) and fixed using a solution of paraformaldehyde and sucrose in PBS (at a final concentration of 4% paraformaldehyde and 2% sucrose in PBS) for 30 min at room temperature. Following fixation, the cells were permeabilized using a solution of 0.3% Triton X-100 in PBS for 15 min at room temperature. For visualization of filamentous-actin (F-Actin) in cells, cells were stained with a solution of Alexa Fluor568-labeled phalloidin (Invitrogen). HCS CellMask Blue (Invitrogen) was used as a fluorescent stain for visualizing nuclei, cytoplasm and the individual cell boundaries. Additional proteins that were

fluorescently labeled and analyzed using appropriate primary antibodies include synaptopodin (synpo), paxillin and vinculin for quantitation of focal adhesions, podocin, and total and activation-dependent epitopes of integrin β1. Appropriate secondary antibodies (fluorescently labeled) were used for fluorescent visualizations. High throughput confocal microscopy was done using the Opera LX (Perkin Elmer) with filters and exposure times according to manufacturer's instructions. Images were used in subsequent image analysis for quantitation of a variety of cellular parameters. Assays were performed in replicate wells for assay robustness.

Image analysis

Images acquired using the HCS Opera imaging system were analyzed using Acapella version 2.0 data processing software (PerkinElmer) and the Columbus 2.4.0 HCS image data storage and analysis system (PerkinElmer). Nuclei were detected using the "Find Nuclei" analysis module and the cytoplasm was detected using the "Find Cytoplasm" analysis module. Cellular morphology properties were calculated to determine cellular features, such as cell area and cell roundness, using the "Calculate Morphology Properties" tool. F-actin fibers, synpo fibers, focal adhesions and integrin β1 spots were identified using the "Find Spots" analysis module, and morphology and intensity properties were calculated using computational parameters in the program.

For HCS assay using a multi-parameter algorithm for automated cell partitioning into multiple populations, we used a machine-learning algorithm in

Columbus. The multiparametric analysis uses a quantitative determination of cellular phenotypic parameters, including cell roundness, cell size, F-actin fiber count and intensity values, to determine a weighted score. Cells from positive and negative control wells were manually identified as “healthy” or “damaged” for training the algorithm. The developed algorithm was then applied on independent images of cells to quantify “percent healthy” or “percent damaged” cells in each well.

Chemical library screening

The pharmacologically active compound libraries used in this screen consisted of commercially available compounds from Microsource (Spectrum Collection), ENZO (kinase inhibitor panel), Sigma, Millipore, Tocris and Cayman and is described in Table I. Stocks of chemicals were prepared in 100% DMSO (2-5 mM) and were arrayed in 96 well plates using PerkinElmer Janus robotic station. Screening of chemical libraries was performed using podocytes cultured in 96-well optical plates (PerkinElmer, Waltham, MA). 100nL of each compound from compound stock plates was added to each well of a podocyte containing 96-well plate using the Perkin Elmer Janus automated workstation with the help of a 96-pin pin tool (100nL, PerkinElmer). The compounds were added in the absence or presence of podocyte damaging agent (such as PAN). The plates containing the compounds were subsequently placed in tissue culture incubators and cells were further cultured for 48h at 37°C. Images from the primary screen were quantified for cell morphology parameter and were normalized by calculating z-score (z) for

each test compound, to compensate for any plate-to-plate variability.[5] z was calculated for each of the test compounds using the formula: $z = \frac{(x-\mu)}{\sigma}$, where x is the raw measured value with each compound, μ is the mean of all measured raw values across a plate and σ is the standard deviation of the measurements. A z-score of |1.28|, corresponding to 90% population under the curve, was used as a cutoff to identify primary hits in the assay.

Scratch, wound-healing assay

The effect of identified novel compounds on podocyte migration was assessed using a classic scratch, wound-healing assay as described.[6] Differentiated mouse podocytes per well were seeded overnight in type-I collagen coated wells of a 24 well plate. Each well was subsequently scratched using a sterile 200 μl pipette tip, washed and placed into fresh culture medium. Cells in wells were also treated with PAN, LPS, pyr or a combination, as described in the text. After 48h, cells were fixed with 2% paraformaldehyde and stained with DAPI. Images of cells near scratched surfaces and their DAPI-stained nuclei were acquired using a 10× objective using a Zeiss Axio Observer D1 microscope (Carl Zeiss Group, Hartford, Connecticut) and analyzed using ImageJ software (NIH). Images using transmitted light were also acquired at the beginning and the end of the experiment and were used to align images of pre- and post-treated cells for counting cells that had migrated into similar sized fields. The data shown represent the mean ± SEM of three independent experiments.

LPS-induced proteinuria

The induction of proteinuria in female wild type C57BL/6J mice (n=6-13 per group) by LPS injection was performed as described.[7-10] Briefly, 10 week old female mice were intraperitoneally injected with LPS (10 mg/kg, in saline). Control mice were injected with saline alone. Animals in the treatment groups were treated with vehicle or 10mg/kg pyr (stock in DMSO) diluted in saline 2h prior to the administration of LPS. Spot urine was collected from each group of animals for measurement of albuminuria as mg albumin per mg creatinine.[9] Results are expressed as mean ± SEM. The mice were sacrificed and the efficacy of pyrintegrin was further analyzed by histochemical and immunofluorescence analyses.

PAN-induced nephropathy

The induction of nephropathy in male wild type SD rats (n = 6 per group) by PAN injection was performed as described.[7, 11, 12] Briefly, 5 week old male rats were intravenously injected with PAN (150 mg/kg, in water) and treatment with vehicle or pyrintegrin was started on the same day. Animals in the vehicle group were administered saline-based vehicle solution (3.3% DMSO and 5% Cremaphor EL) intraperitoneally daily for 14 days. Animals in the treatment group were treated with pyrintegrin (10mg/kg, 3.3% DMSO and 5% Cremaphor EL) in the saline based solution daily for 14 days. Spot urine was collected from animals for measurement of albuminuria as mg albumin per mg creatinine.[9] Results are expressed as mean ± SEM.

Light and electron microscopy

For light microscopy, freshly harvested mouse kidney tissue was embedded in OCT, snap frozen in liquid nitrogen and stored at -80°C. Tissue sections were cut and fixed in -20°C acetone before immunofluorescence staining. Sections were blocked at room temperature for 1h and incubated with the primary antibodies against total β1 integrin (hamster anti-mouse, BioLegend), active β1 integrin[1] (rat anti-mouse antibody 9EG7, BD Biosciences) and synaptopodin (polyclonal goat, SC-21537, Santa Cruz) at 4°C overnight. Slides were incubated with appropriate fluorescently labeled secondary antibodies (Life Technologies, CA) and mounted with DAPI containing mounting solution (Vector Laboratories, Burlingame, CA). Fluorescence images were acquired using a Zeiss 700 LSM confocal microscope with a 20X objective and analyzed using the Zen software (Carl Zeiss Group, Hartford, Connecticut).

For transmission electron microscopy (TEM), tissues were fixed, embedded, sectioned, and stained as previously described.[11] Images were acquired using Zeiss SIGMA HD VP electron microscope.

Statistical analysis

Data were analyzed using PerkinElmer Columbus and GraphPad Prism software and were compared with using the Student's *t*-test, where appropriate. $P < 0.05$ was considered statistically significant. Z'-value (Z-prime value), a measure of statistical effect size to determine if the assay response is significant, was calculated as described in literature.[13]

B. Supplementary Table

Table S1. Small molecule chemical compounds used in the HCS assay with podocytes. List of chemical libraries used in the current HCS assay.

C. Supplementary Figures

Figure S1. Cell cultured in 96-well optical plates for HCS assays express typical markers of healthy podocytes.

Figure S2. Dexamethasone (DEX) dose-dependently protects podocyte from PAN injury.

Figure S3. HCS assay using a multi-parameter algorithm also shows low variability.

Figure S4. Chemical screening data shows bell shaped curve.

Figure S5. Images of cells from the assay wells of the primary screen.

Figure S6. Images of murine podocytes showing that pyrintegrin (pyr) protects podocytes from PAN-induced damage.

Figure S7. Pyrintegrin (pyr) protects podocytes from LPS-induced loss of F-actin fibers and enhances integrin $\beta 1$.

Figure S1. Cell cultured in 96-well optical plates for HCS assays express typical markers of healthy podocytes. **A.** Representative images of single frames from a 96-well plate showing podocytes cultured in optical plates and stained with HCS CellMask blue (top panels) and antibodies against synaptopodin, podocin or integrin β1 (bottom panels). Images were acquired using PerkinElmer Opera high-content screening microscope. Scale bar, 50 μm. **B.** A graph showing the quantification of the number of nuclei in each of the 48 wells of a plate. Podocytes were cultured in 48 replica wells of a 96-well optical plate, as described in the methods section. Cells in each well were stained with CellMask Blue, which also stains the nuclei. Wells were imaged using Opera HCS system and nuclei in each well were automatically counted. The graph shows that podocytes cultured in multi-well plates show low well-to-well variability in cell number.

Figure S2. Dexamethasone (DEX) dose-dependently protects podocyte from PAN injury. Podocytes in 96-well optical plates were co-treated with PAN (30 μg/mL) and an increasing concentration of DEX at 37°C for 48h and the cellular damage was assessed using HCS system. **A**. A dose-response curve showing the protective effects of increasing concentration of DEX on F-actin fiber count per cell. Data shown are means ± the standard error of the mean (SEM) per cell from a single assay well (n = 500-1000 cells), performed in three replicate wells. **B**. Representative fluorescence images of cells co-treated PAN (30 μg/mL) and an increasing dose of DEX (as shown) and stained with CellMask Blue and phalloidin are shown. Scale bar, 50 μm.

Figure S3. HCS assay using a multi-parameter algorithm shows low variability. Podocyte health and damage can be quantified using a combination of cellular parameters that were measured by Opera and Columbus. A machine-learning algorithm was used to segregate cells in each well into “percent healthy” or “percent damaged” and plotted in this dose-response series. **A**. Representative images after processing with a multiparameter algorithm showing phalloidin stained cells (top panel) after treatment with various doses of PAN and PAN + MZR, as indicated. Cells automatically identified by the machine-learning algorithm as “damaged” in each image frame are colored red in the bottom panel. Scale bar, 50 μm. **B**. Dose-response curves using “percent damaged” algorithm showing a dose-dependent increase in podocyte damage with PAN (left) or a dose-dependent decrease in podocyte damage with PAN and MZR co-treatment (right). Each data point represents results from three replicated wells. **C**. A graph showing analysis of assay variability of the newly developed podocyte cell-based assay and analyzed using the automated multi-parameter algorithm for “percent damaged” cells under each condition (n = 500-1000 cells/well) and the calculated mean ± 95% confidence intervals across 30 wells. The calculated Z'-value between cells treated with PAN alone (damaged) or healthy cells (control) is also shown. **** $p<0.0001$.

Figure S4. Chemical screening data shows bell shaped curve. **A**. A frequency plot showing the distribution of total nuclei count per assay well (x-axis) from the primary assay (bin width = 50) versus the number of compounds or wells (frequency) in each bin of the nuclei count on y-axis. **B**. A frequency plot showing the distribution of z-score values (bin width = 0.1) from the primary assay versus the number of compounds or wells (frequency) in each bin of the z-score on y-axis.

Figure S5. Images of cells from wells of selected hits from the primary screen show protection from PAN injury. Representative CellMask Blue stained fluorescence images from primary screen showing (**A**) control cells treated with PAN alone or PAN + MZR (as shown), or (**B**) cells co-treated with PAN and the indicated compound. Scale bar, 50 μm.

Figure S6. Images of murine podocytes showing that pyrintegrin (pyr) protects podocytes from PAN-induced damage. Podocytes in 96-well optical plates were cultured at 37°C for 48h in the absence (Control, Con) or presence of PAN (30 μg/mL) and co-treated with vehicle (DMSO, 1%) or pyrintegrin (pyr) (1 μM). The cellular damage was assessed after staining the cells with phalloidin, anti-paxillin and anti-integrin β1 antibodies and quantifying various cellular phenotypes using the HCS system. The panel here shows representative fluorescence images of the cells. Two color co-stained images show cells stained with phalloidin (red) and anti-paxillin antibody (green) (central panels) or phalloidin (red) and anti-integrin β1 antibody (green) (right panels). Images were acquired using a confocal microscope. Scale bar, 50 μm.

Figure S7. Pyrintegrin (pyr) protects podocytes from LPS-induced damage. Podocytes in 96-well optical plates were cultured at 37°C for 48h in presence of LPS (100 μg/mL) and co-treated with vehicle (DMSO, 1%) or pyr (1 μM) and the cellular damage was assessed after staining the cells with phalloidin, anti-paxillin or anti-vincullin and anti-β1 antibodies and quantifying various cellular phenotypes using the HCS system. **A**. Representative fluorescence images of murine podocytes after various treatments, as described in panel **B** and shown on the left side of the images, and after staining with phalloidin, anti-paxillin or anti-β1 antibodies. Two color co-stained images show cells stained with phalloidin (red) and anti-paxillin antibody (green) (central panels) or phalloidin (red) and anti-β1 antibody (green) (right panels). Images were acquired using the Opera HCS system. Scale bar, 50 μm. **B.** Graphs showing the effect of pyrintegrin on the number of F-actin fibers per cell and the integrin β1 spots per cell under each treatment condition are presented. Data shown are means ± SEM per cell from three replicate wells (n = 500-1000 cells/well). *$p < 0.05$.

D. Supplementary References

1. Lenter, M, Uhlig, H, Hamann, A, Jeno, P, Imhof, B, Vestweber, D: A monoclonal antibody against an activation epitope on mouse integrin chain beta 1 blocks adhesion of lymphocytes to the endothelial integrin alpha 6 beta 1. *Proc Natl Acad Sci U S A,* 90**:** 9051-9055, 1993.

2. Alachkar, N, Carter-Monroe, N, Reiser, J: Abatacept in B7-1-positive proteinuric kidney disease. *The New England journal of medicine,* 370**:** 1263-1264, 2014.

3. Mundel, P, Reiser, J, Zuniga Mejia Borja, A, Pavenstadt, H, Davidson, GR, Kriz, W, Zeller, R: Rearrangements of the cytoskeleton and cell contacts induce process formation during differentiation of conditionally immortalized mouse podocyte cell lines. *Experimental cell research,* 236**:** 248-258, 1997.

4. Saleem, MA, O'Hare, MJ, Reiser, J, Coward, RJ, Inward, CD, Farren, T, Xing, CY, Ni, L, Mathieson, PW, Mundel, P: A conditionally immortalized human podocyte cell line demonstrating nephrin and podocin expression. *Journal of the American Society of Nephrology : JASN,* 13**:** 630-638, 2002.

5. Zhang, XD: Illustration of SSMD, z score, SSMD*, z* score, and t statistic for hit selection in RNAi high-throughput screens. *Journal of biomolecular screening,* 16**:** 775-785, 2011.

6. Asanuma, K, Yanagida-Asanuma, E, Faul, C, Tomino, Y, Kim, K, Mundel, P: Synaptopodin orchestrates actin organization and cell motility via regulation of RhoA signalling. *Nat Cell Biol,* 8**:** 485-491, 2006.

7. Reiser, J, von Gersdorff, G, Loos, M, Oh, J, Asanuma, K, Giardino, L, Rastaldi, MP, Calvaresi, N, Watanabe, H, Schwarz, K, Faul, C, Kretzler, M, Davidson, A, Sugimoto, H, Kalluri, R, Sharpe, AH, Kreidberg, JA, Mundel, P: Induction of B7-1 in podocytes is associated with nephrotic syndrome. *J Clin Invest,* 113**:** 1390-1397, 2004.

8. Yanagida-Asanuma, E, Asanuma, K, Kim, K, Donnelly, M, Young Choi, H, Hyung Chang, J, Suetsugu, S, Tomino, Y, Takenawa, T, Faul, C, Mundel, P: Synaptopodin protects against proteinuria by disrupting Cdc42:IRSp53:Mena signaling complexes in kidney podocytes. *The American journal of pathology,* 171**:** 415-427, 2007.

9. Faul, C, Donnelly, M, Merscher-Gomez, S, Chang, YH, Franz, S, Delfgaauw, J, Chang, JM, Choi, HY, Campbell, KN, Kim, K, Reiser, J, Mundel, P: The actin cytoskeleton of kidney podocytes is a direct target of the antiproteinuric effect of cyclosporine A. *Nature medicine*, 2008.

10. Yu, CC, Fornoni, A, Weins, A, Hakroush, S, Maiguel, D, Sageshima, J, Chen, L, Ciancio, G, Faridi, MH, Behr, D, Campbell, KN, Chang, JM, Chen, HC, Oh, J, Faul, C, Arnaout, MA, Fiorina, P, Gupta, V, Greka, A, Burke, GW, 3rd, Mundel, P: Abatacept in B7-1-positive proteinuric kidney disease. *The New England journal of medicine,* 369**:** 2416-2423, 2013.

11. Wei, C, Moller, CC, Altintas, MM, Li, J, Schwarz, K, Zacchigna, S, Xie, L, Henger, A, Schmid, H, Rastaldi, MP, Cowan, P, Kretzler, M, Parrilla, R, Bendayan, M, Gupta, V, Nikolic, B, Kalluri, R, Carmeliet, P, Mundel, P, Reiser, J: Modification of kidney barrier function by the urokinase receptor. *Nature medicine,* 14**:** 55-63, 2008.

12. Nakamura, T, Ebihara, I, Shirato, I, Tomino, Y, Koide, H: Modulation of basement membrane component gene expression in glomeruli of aminonucleoside nephrosis. *Laboratory investigation; a journal of technical methods and pathology,* 64**:** 640-647, 1991.

13. Zhang, JH, Chung, TD, Oldenburg, KR: A Simple Statistical Parameter for Use in Evaluation and Validation of High Throughput Screening Assays. *Journal of biomolecular screening,* 4**:** 67-73, 1999.

Table S1. Small molecule chemical compounds used in the HCS assay with podocytes

Library	Vendor/Source	Number of compounds
The spectrum collection	Microsource Discovery Systems	2000
Protein Kinase Inhibitor Library	Enzo	80
*Selected small molecules	Tocris/Cayman etc	41
Total		2121

*These compounds were selected in-house from various commercial sources

A

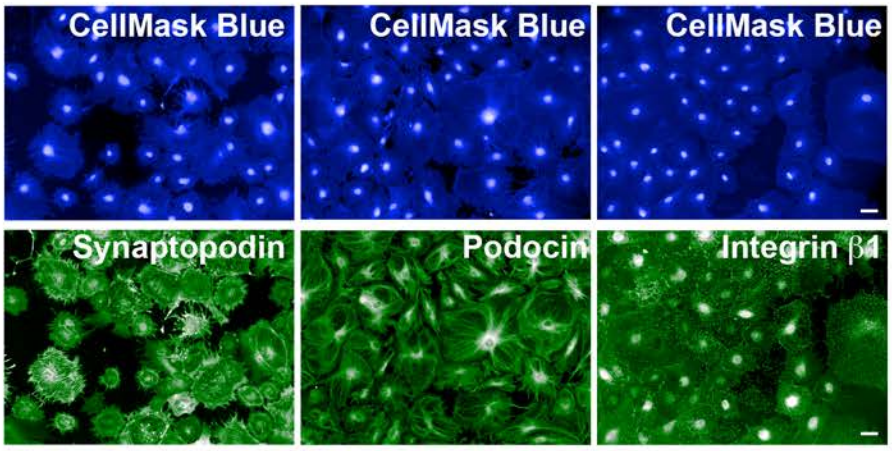
CellMask Blue
CellMask Blue
CellMask Blue
Synaptopodin
Podocin
Integrin β1

B

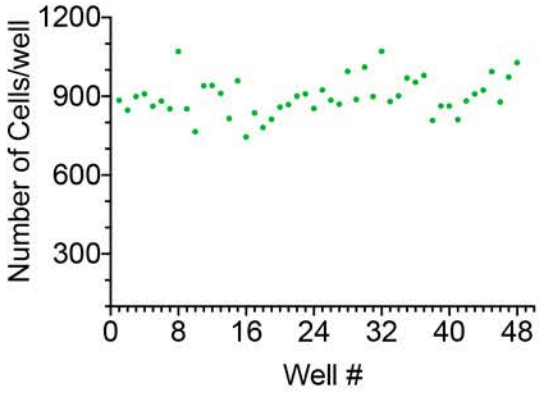
Number of Cells/well
1200
900
600
300
0
8
16
24
32
40
48
Well #

Figure S1

A

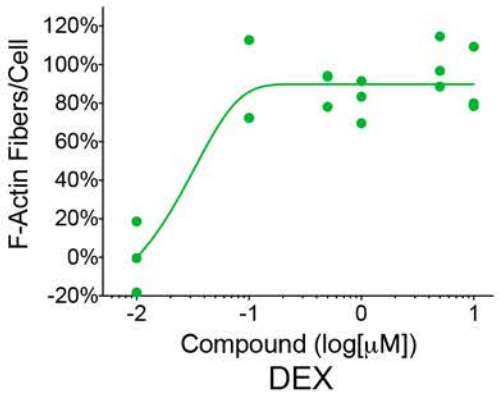
F-Actin Fibers/Cell
120%
100%
80%
60%
40%
20%
0%
-20%
-2
-1
0
1
Compound (log[μM])
DEX

B

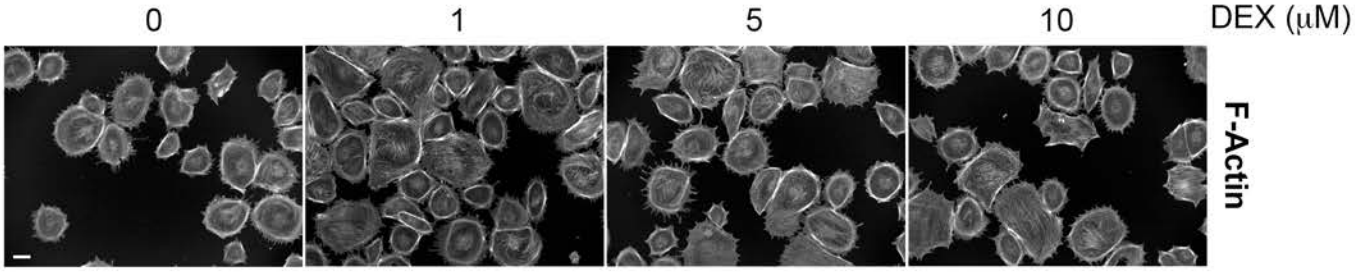
0
1
5
10
DEX (μM)
F-Actin

Figure S2

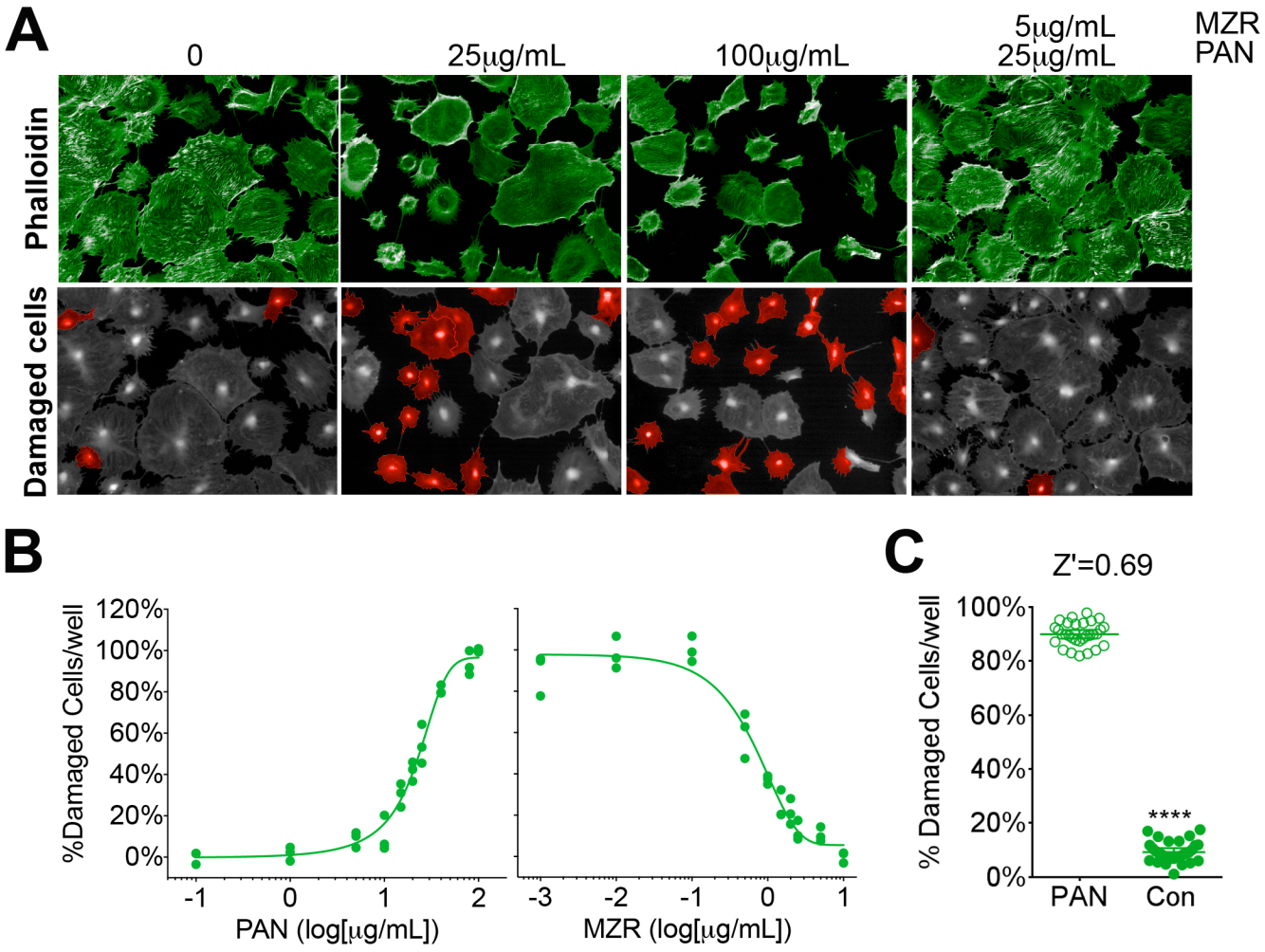
A
0
25μg/mL
100μg/mL
5μg/mL
25μg/mL
MZR
PAN
Phalloidin
Damaged cells
B
%Damaged Cells/well
120%
100%
80%
60%
40%
20%
0%
-1
0
1
2
PAN (log[μg/mL])
-3
-2
-1
0
1
MZR (log[μg/mL])
C
Z'=0.69
% Damaged Cells/well
100%
80%
60%
40%
20%
0%
****
PAN
Con

Figure S3

A

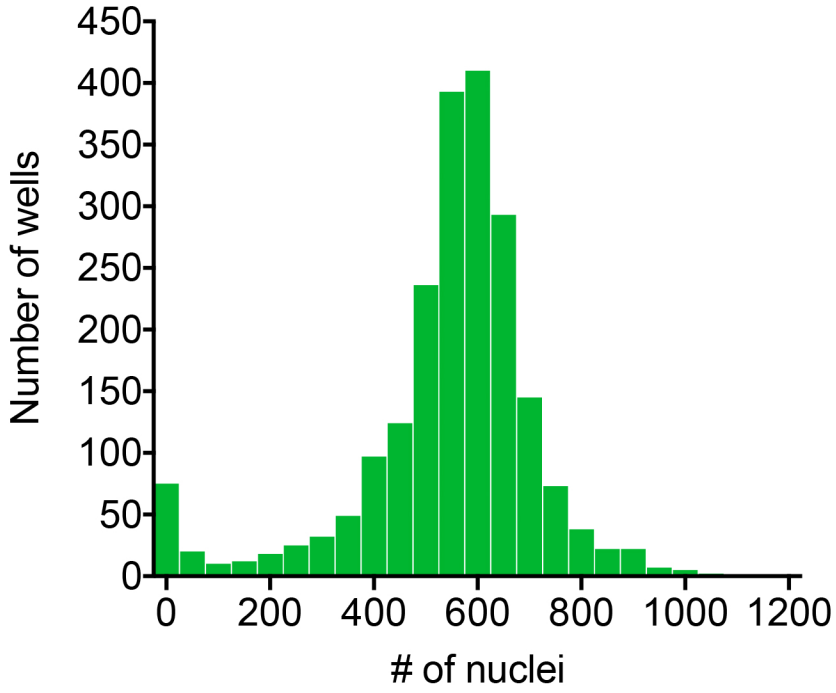
Number of wells
450
400
350
300
250
200
150
100
50
0
0
200
400
600
800
1000
1200
# of nuclei

B

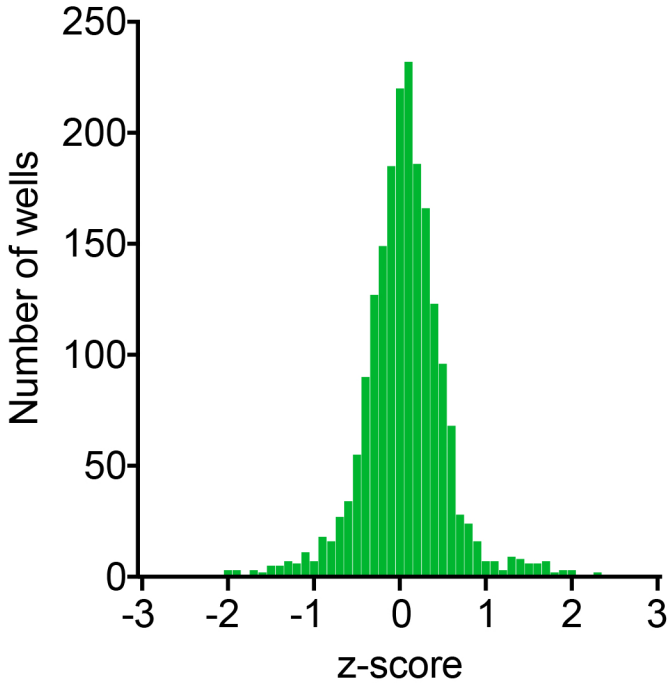
Number of wells
250
200
150
100
50
0
-3
-2
-1
0
1
2
3
z-score

Figure S4

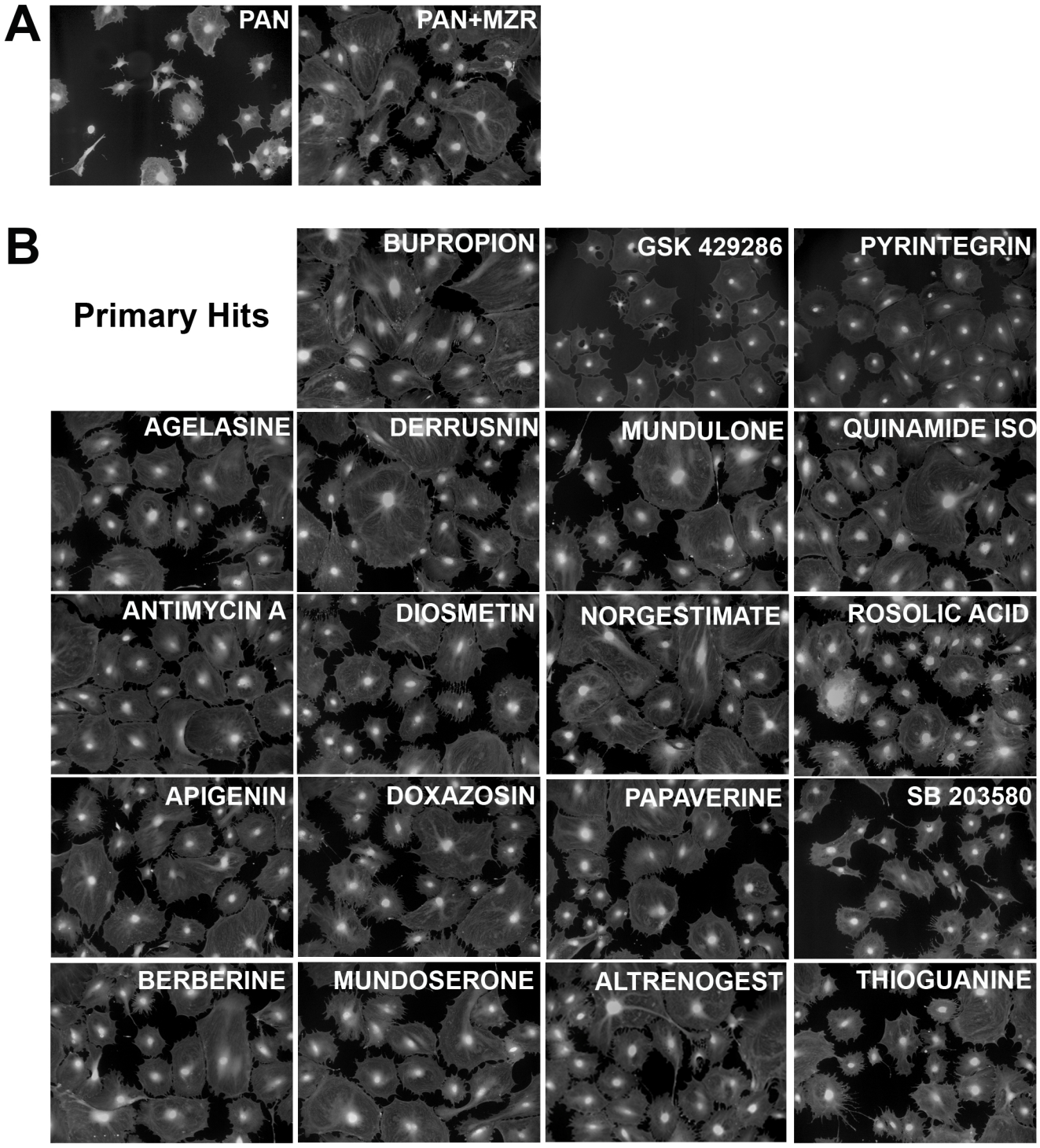
A
PAN
PAN+MZR
B
Primary Hits
BUPROPION
GSK 429286
PYRINTEGRIN
AGELASINE
DERRUSNIN
MUNDULONE
QUINAMIDE ISO
ANTIMYCIN A
DIOSMETIN
NORGESTIMATE
ROSOLIC ACID
APIGENIN
DOXAZOSIN
PAPAVERINE
SB 203580
BERBERINE
MUNDOSERONE
ALTRENOGEST
THIOGUANINE

Figure S5

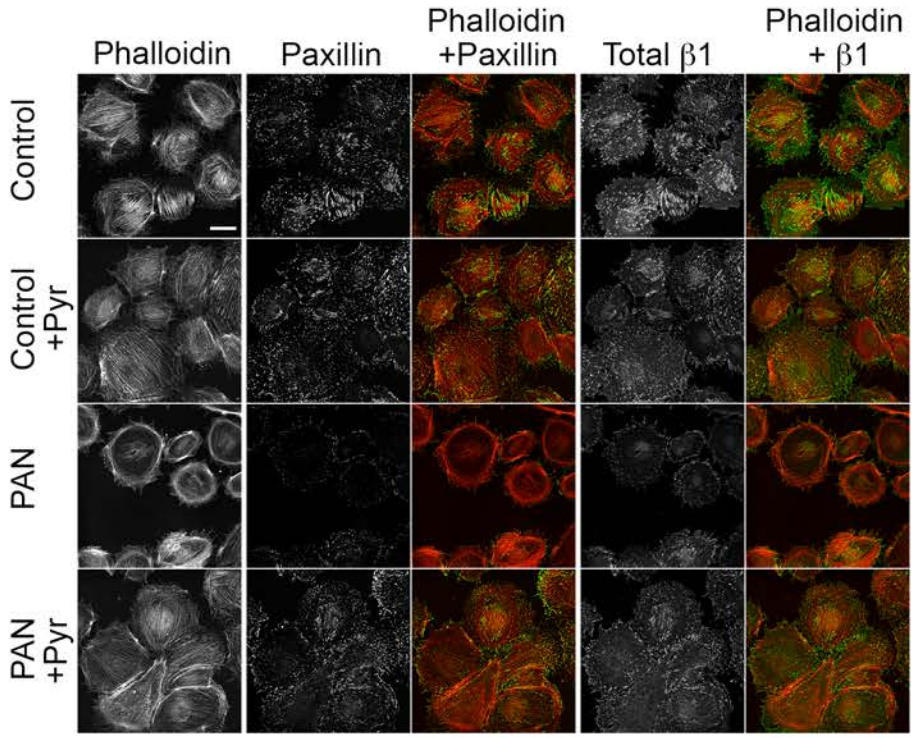
Phalloidin
Paxillin
Phalloidin +Paxillin
Total β1
Phalloidin + β1
Control
Control +Pyr
PAN
PAN +Pyr

Figure S6

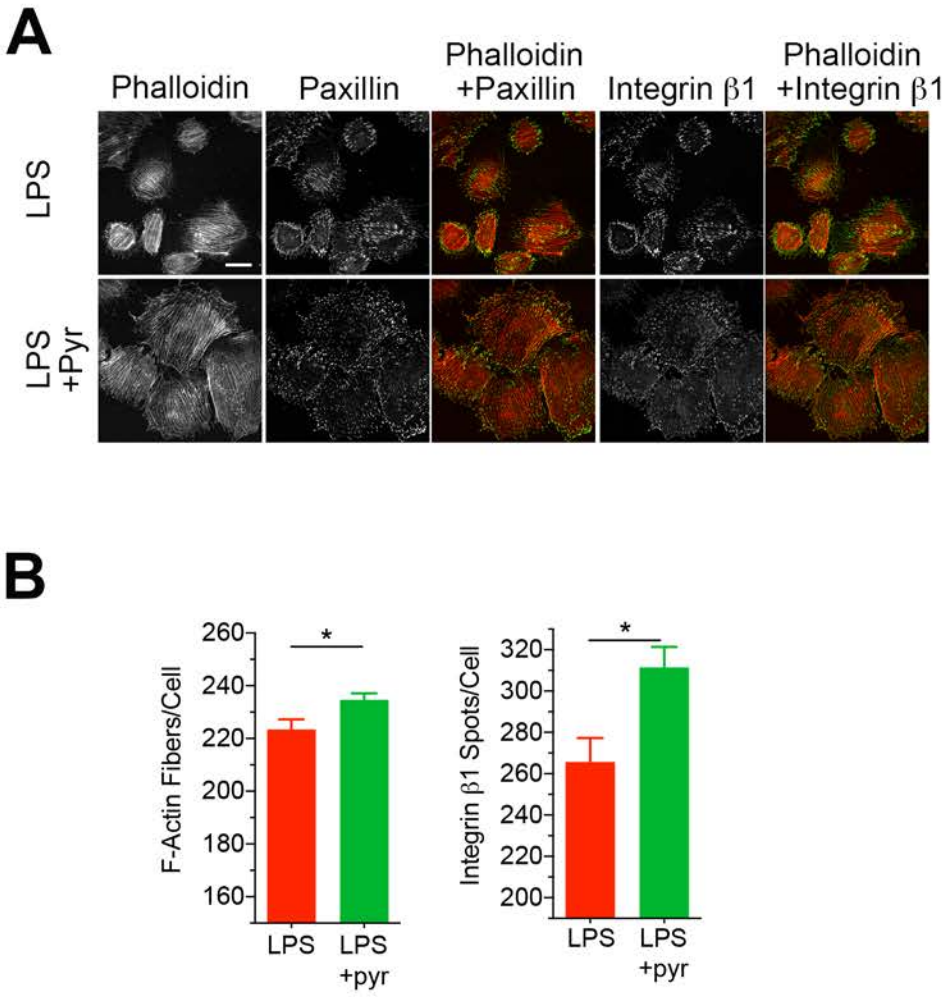
A
Phalloidin
Paxillin
Phalloidin +Paxillin
Integrin β1
Phalloidin +Integrin β1
LPS
LPS +Pyr
B
F-Actin Fibers/Cell
260
240
220
200
180
160
*
LPS
LPS +pyr
Integrin β1 Spots/Cell
320
300
280
260
240
220
200
*
LPS
LPS +pyr

Figure S7